

## APPLICATION OF THE ANALYTICAL HIERARCHY PROCESS (AHP) FOR LANDSLIDE SUSCEPTIBILITY MAPPING IN THE EAST REGION OF CONSTANTINE, NE ALGERIA.

Submitted on 25/04/2018 – Accepted on 07/11/2018

### Abstract

Landslides constitutes one of the main geological dangers to human being. Proper analysis and suitable modeling of these dangers may reduce accident risks. In this study, we used remote sensing techniques and GIS tools to establish landslide susceptibility map of the East of Constantine. To evaluate the landslide risks in the study area, analytical hierarchy process (AHP) method and Weighted Linear Combination (WLC) were used. In this method, we performed quantification of the factors on a priority basis by pair-wise comparison of the factors. The local data includes slope, slope aspect, elevation, distance from drainage, lithology, distance from faults, precipitation, and Normalized Difference Vegetation Index (NDVI) and springs density. The landslide susceptibility index (LSI) was calculated using the WLC technique based on the assigned weight and rating by AHP method. The results were verified using actual landslide locations (43 location points) where the accuracy rate 61% of predict values and 58 % of success values. The validation results with that indicated suitable agreement between the susceptibility map and the existing data on landslide locations.

**Keywords:** Landslides, Susceptibility, AHP, GIS, Mapping, Constantine.

**N MANCHAR**<sup>1</sup>  
**CH BENABBAS**<sup>2</sup>  
**F BOUAICHA**<sup>3</sup>  
**K BOUFAA**<sup>4</sup>

<sup>1</sup> Department of geology sciences, University of Freres Mentouri Constantine, Algeria.

<sup>2</sup> Geology and environment laboratory (L.G.E), University of Constantine 3, Algeria.

<sup>3</sup> Department of applied biology, university of Frères Mentouri Constantine 1, Constantine, Algeria.

<sup>4</sup> Laboratory of Geological Engineering (L.G.G), University of Jijel, Algeria.

### INTRODUCTION

Landslides are destructive natural hazards that frequently leads to serious problems. In northern Algeria, the Constantine's region in particular, East of the city is severely affected by recurrent landslides causing damage to property and infrastructure ([1]; [2]; [3]; [4]; [5]; [6]; [7]; [8]). To the East of the city, a 10 Km segment of East-West highway experienced many landslides during construction. This segment is hosting two tunnels (Djebel Ouahche's tunnel and Kellal's tunnel) near which several landslides and instabilities occurred especially in Dj Ouahche. The most recent landslides occurred in 2008, 2011, and 2013 caused serious damage to the highway's infrastructures; such as the tunnel of Djebel Ouahche, and embankment of the highway.

Landslide susceptibility zonation (LSZ) is defined as dividing land areas into homogeneous domain based on their potential landslide occurrence ([9]; [10]; [11]). LSZ was developed by a variety of methods and techniques which are carried out into two approaches: (i) a qualitative approach that is based on expert knowledge of the target area and portrays susceptibility zoning in descriptive terms; and (ii) a quantitative approach based on statistical algorithm ([12]; [13]; [14]; [15]; [16]; [17]; [18]).

Recently, quantitative approaches are commonly used. It is based on mathematical expressions of the relationship between causal factors and the landslides. The two principles methods for quantitative analysis are the deterministic and

statistical method, which includes multivariate and bivariate statistical models, Fuzzy logic, logistic regression and artificial neural network analysis ([19]; [13]; [20]; [21]; [22]; [23]). Deterministic methods are based on engineering principles of slope instability defined in terms of the factor of safety. However these methods are useful for mapping only small areas.

The qualitative approach is based on expertise reports for which a landslide inventory map is not necessary. Maps resulting from quantitative techniques are influenced by the subjectivity of the experts involved.

The Analytical Hierarchy Process (AHP) is a semi-quantitative method. It is based on decomposition, the comparison between different pairs of elements, and synthesis of priorities for regional susceptibility studies. This method was introduced by [36] Saaty (1980) and depends on the expert knowledge ([24]; [25]). In this study, AHP along with GIS are powerful instruments to inspect criteria in modelling process.

The purpose of this research is to present landslide susceptibility map for the east of Constantine city (Northeast of Algeria), using AHP method in the framework of GIS.

### 2. GEOLOGICAL AND GEOMORPHOLOGICAL SETTINGS

The study area is located in the Northeast of Algeria. It concerns the zoning perimeter with 1/50 000 scale

(geological map of Algeria; map N°74 EL ARIA), covering an area of about 639.56 km<sup>2</sup>. This region is affected by several landslides, due to its geological and geomorphological particularities. Also, the anthropogenic factors are responsible for many landslides triggering in the area such as roads, highways and tunnels.

The geomorphology of Constantine region is particular in Tellian Atlas Mountains of northeast Algeria with deep gorges (Rhumel, Rocher de Constantine) and mountains (Dj Kellal “950 m”, Kef El Akahl “1200 m”, Dj Ouahche “1100 m”). The altitude ranges from 500 m to 1200 m. The area characterized by a dense hydrographic network with main draining valleys such as Oued Boumerzoug, Oued Hamimin, Oued Bousteila in the west and Oued El Kram, Oued El Aria and Oued en Naga in the east which have permanent flow. However, the temporary flow presented by Oued El Anga, Oued El Mellah and Oued Boudeb, often these streams are flowing to the Northeast direction.

The study area is characterized by a semi-arid climate with high temperature (28 -41°C) and low precipitation (from 600 to 900 mm) in the summer, and high humidity, precipitation and low temperature in the winter. Two typical rainy and dry seasons are in contrast. About 63% of the annual rainfall quantity concentrated between Decembers to February period. The rainstorm represents the triggering factor for most of landslides.

Geologically, the study area is characterized by superposition of thrust sheet units made up from the base to the top (Fig. 1) by:

Neritic unit (Cretaceous carbonate), Ultra-Tellian unit (Cretaceous-Eocene marls and marly limestone), Tellian s.s. (sensu-structo) with Marly dominance (Cretaceous-Eocene), Numidian unit with sandstone Burdigalian, clay and flysch (Eocene), and Mio-Plio-Quaternary formations which are represented by sandy clays, marls and conglomerate (Mio-Pliocene) and alluvial terraces and lacustrine calcareous formations with Quaternary age ([26]; [27]; [28]; [29]; [30]). This edifice was deposited during paroxysmal compressional phases Eocene and Miocene ([26]; [31]; [32]; [30]).

### 3. METHODOLOGY AND ANALYSIS

The instability complexity at this site is results of the combination of several factors that may or may not act synchronously. Nine possible landslide causative factors such as slope, slope aspect, elevation, distance from drainage, lithology, distance from faults, precipitation, NDVI and springs density were used. These factors were analyzed and taken into account to procedure landslide susceptibility of the study area. The layers were generated from the various data sources.

#### 3.1. Data presentation and analysis

The data used in the present study are satellite image (Landsat-7 ETM satellite images (Resolution 30 m), aerial photo, geological map and topographical map (Table 1).

The contour map at 10 m interval was prepared and digitized from Constantine’s topographical map (1980) at the scale 1/50000 and subsequently employed for generating the DEM

using GIS software. Elevation, slope, and slope aspect were extracted from DEM with 10 m grid cell size (Fig. 2a, b, c). Slope gradient with seven classes, slope aspect, was classified into the eight known main direction. Seven main lithological classes and transformed into raster value domain on GIS software (Fig. 2g). The class weight value for each strength was identified and described by GIS. Drainage buffering map was made on the distances interval 200 m from the topographic map at the 1/25000 scale and classified with ten intervals (Fig. 2e). The precipitation is considered as the most common trigger of landslides ([33]; [34]). Five hydro-climatic stations such as Constantine, Hamma Bouziane, Ain El Bey, Fourchi and Bir Drimil of the **Agence Nationale des Ressources Hydrauliques (ANRH, Algiers)**, and the **Office National de Météorologie (ONM, Algiers)** was selected. The precipitation values was used to create the precipitation map during 32 years (1980-2012) (Fig. 2, i). Fault buffering was made on a distance interval of 400 m from the geological map at the 1/50000 scale and classified with ten intervals. Spring water layer was extracted from the topographical map at the 1/50000 scale (Fig. 2, d). The NDVI map was created from Landsat-7 TM satellite images (Resolution 30 m) (Fig. 2, f). The prepared NDVI by a non-linear transformation of the visible or red and near-infrared bands of satellite images [35]. It can be calculated using the formula:

$$NDVI = (NIR - R) / (NIR + R) \quad (1)$$

Where NIR and R are the observed reflectance in the near infrared and red portions of the electromagnetic spectrum, respectively. The values were ranged from -1 to +1 (pixel values 0-255) (Fig. 2).

#### 3.2. Methodology

In the present research, the AHP technique was applied and the Weighted Linear Combination (WLC) was performed by integrating factors weight and class weight/ rank value to compute landslide susceptibility index (LSI) for each pixel:

$$LSI = \sum_{i=1}^n (W_i * R_i) \quad (2)$$

Where LSI is the required landslide susceptibility index of the given pixel, Ri and Wi are class weight.

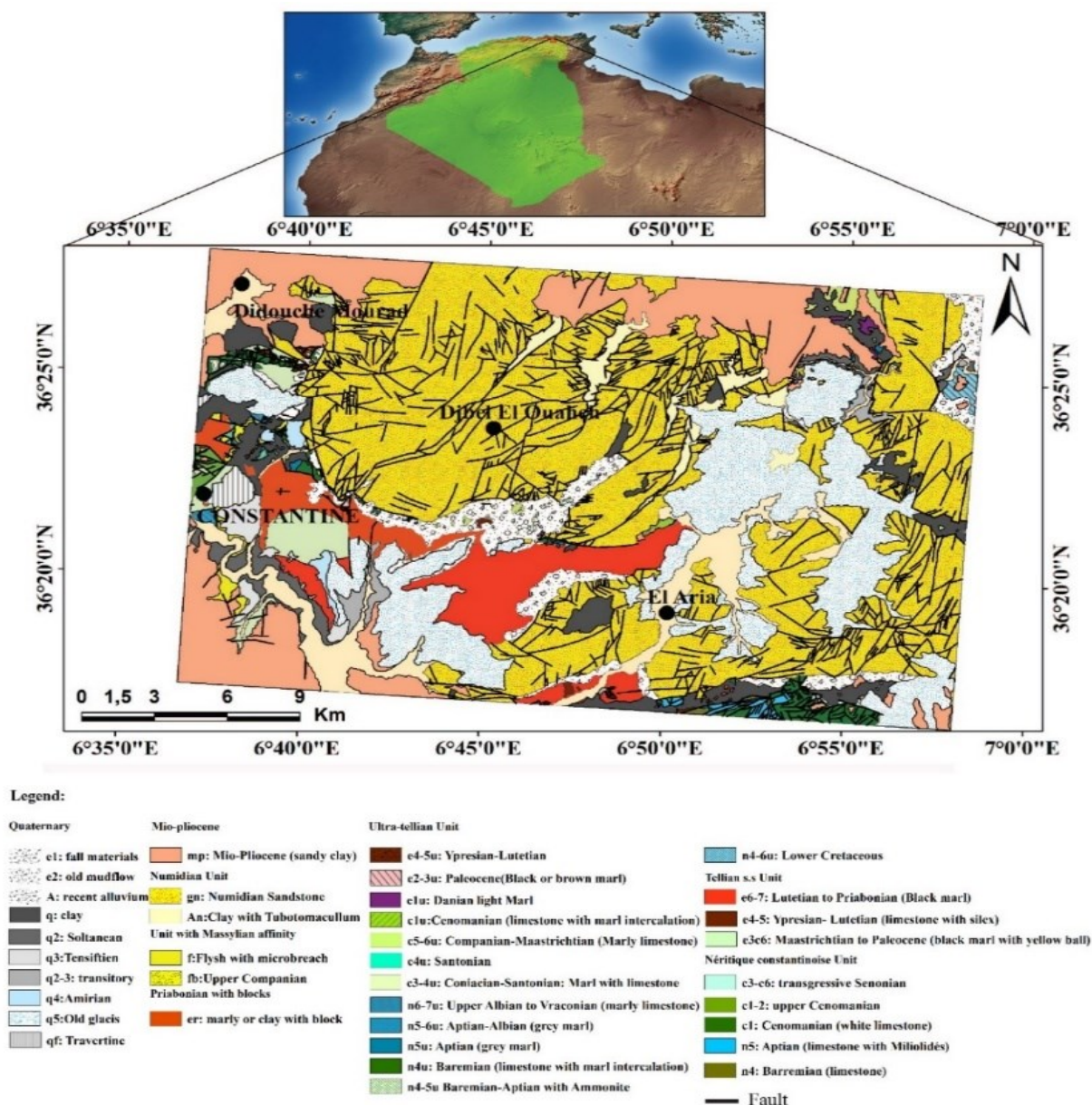


Fig. 1: Geological map of Study area, after Coiffait and Vila, 1977 (modified).

Table. 1 Spatial data layers used in the study.

Category	Layer	Data type	Scale	Data Source
Topographic map	MNT	GRID & point	1/50000	I. N. C. T. (Institut National de la Cartographie et de Télédetection)
	hypsoetry			
	Slope angle			
	Slope aspect			
	Water springs			
Topographic map	Distance from drainage	Polygone	1/25000	A. N. G. C. M. (Agence Nationale de la Géologie et du Contrôle Minier)
Geological map	Lithology	Polygone	1/50000	
	Distance from fault			ANRH (Agence National des Ressources Minérales)
Precipitation map	Precipitation	GRID	1/50000	
NDVI map	NDVI	GRID	30m x30m	Landsat-7 ETM+ Satellite image (scene P193R35, year 2001)



Table 2: Scale of preference between two parameters in AHP (Saaty, 2000)

Scale	Degree of preferences	Explanation
1	Equally	Two activities contribute equally to the objective,
3	Moderately	Experience and judgement slightly to moderately favor one activity over another
5	Strongly	Experience and judgement strongly or essentially favor one activity over another
7	Very Strongly	An activity is strongly favored over another and its dominance is showed in practice
9	Extremly	The evidence of favoring one activity over another is of the highest degree possible of an affirmation.
2,4,6,8	Intermediate Values	Used to represent compromises between the preferences in weights 1, 3, 5, 7 and 9.
Reciprocals	Opposites	Used for inverse comparison.

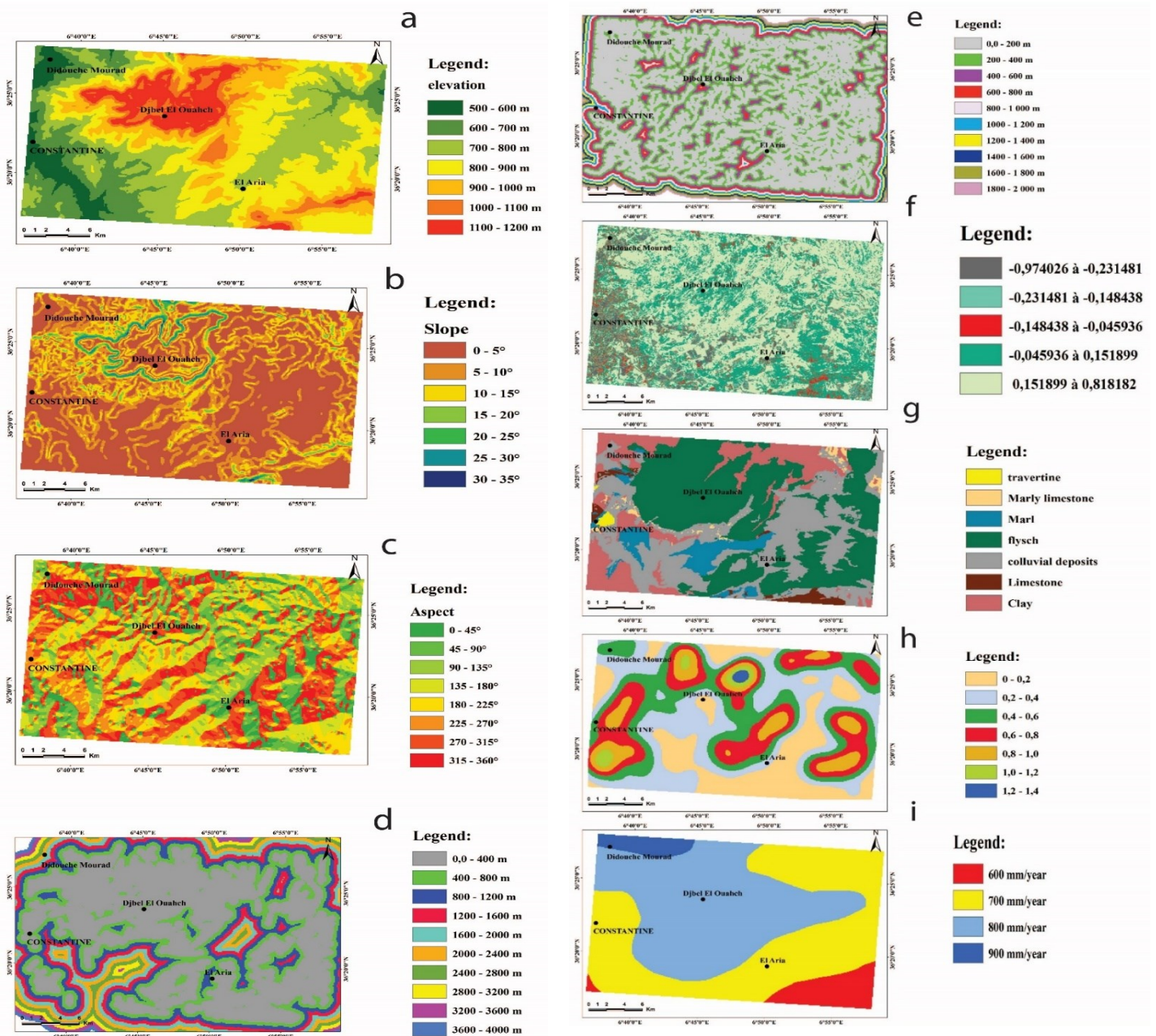


Fig. 2 Landslide related factors in the study area: (a) elevation (b) Slope angle (c) Slope aspect (d) distance from faults (e) distance from drainage (f) NDVI (g) Lithology (h) density of springs (i) precipitation

**Analytical Hierarchy Process**

The analytical hierarchy process (AHP) is a semi-quantitative and multicriteria decision-making method, enables to organize, analyze, and can find an answer to a complex decision problem [36]. This approach is based on three principles: decomposition, comparative judgment, and synthesis of priorities [37]. It involves a matrix-based pair-wise comparison of the decomposed elements inside a given level of hierarchical structure with respect to the following higher level (Table 2). By building a pair-wise comparison matrix with scores which are providing in a fundamental numerical scale, range between 1 and 9, to get factor weights. In the construction of a pair-wise comparison matrix, each factor is rated against every other factor using that scale. Then, in order to calculate the final weight for each conditioning factor, the per-wise comparison matrix for each element was generated in the software with a consistency ratio (CR) expressed as:  $CR = (CI/RI)$

Where: RI the consistency index average depending on the order of the matrix given by Saaty (1980). CI is the consistency index expressed as:  $CI = (\lambda_{max} - n) / (n - 1)$ . Where  $\lambda_{max}$  is the largest or principal eigenvalue of the matrix and n is the order of the matrix.

**Geoprocessing**

The aim of the building of per-wise comparison matrix is to get factor weights and class weights, and calculated consistency ratio (CR), is computed to check the construction of matrix which depends on the number of parameters.

The CR value requirement should be less than 0.1 to accept the computed weights. Then the matrix can be considered as having an acceptable consistency [38]. A CR greater than 0.1 were automatically rejected and requires revision of judgment in the matrix.

The required weights were used to calculate the landslide susceptibility. It's made by Weighted Linear Sum procedure [39]. The CR found in this study is 0.00005, the ratio indicates an acceptable value for a reasonable level of consistency into the pair-wise assessment, and validate the factor weights. Therefore, the lithology factor have the highest weights with value of 0.15. However, elevation, distance to fault, and distance to drainage factors have the same lowest values of weights 0.08 (Table. 3).

**Table. 3: The pair-wise comparison matrix, factor weights, class weights (rating) and consistency ratio.**

Factor										
<i>Lithology</i>										
										<i>Weight</i>
9	Clay	1								0.269753
8	Colluvium	0.889	1							0.220726
6	Marl	0.667	0.75	1						0.179833
1	Limestone	0.111	0.125	0.167	1					0.02997
2	Marly-Limestone	0.222	0.25	0.333	2	1				0.059943
3	Travertine	0.333	0.375	0.5	3	1.5	1			0.089916
5	Flysch	0.556	0.625	0.833	5	2.5	1.667	1		0.149859
<i>Consistency Ratio: 0.00882</i>										
<i>Slope aspect</i>										
										<i>Weight</i>
7	0-45°	1								0.159091
5	45-90°	0.714	1							0.113633
1	90-135°	0.143	0.2	1						0.022725
1	135-180°	0.143	0.2	1	1					0.022725
5	180-225°	0.714	1	5	5	1				0.113633
7	225-270°	1	1.4	7	7	1.4	1			0.159091
9	270-315°	1.286	1.8	9	9	1.8	1.286	1		0.20455
9	315-360°	1.286	1.8	9	9	1.8	1.286	1	1	0.20455
<i>Consistency Ratio: 0.000059</i>										
<i>Slope angle</i>										

										<i>Weight</i>	
1	0-5°	1									0.026273
3	5-10°	3	1								0.075067
5	10-15°	5	1.667	1						0.131378	
6	15-20°	6	0.333	1.2	1					0.136648	
7	20-25°	7	2.333	1.4	1.167	1				0.183933	
8	25-30°	8	2.667	1.6	1.333	1.143	1			0.210209	
9	>30°	9	3	1.8	1.5	1.286	1.125	1		0.236491	
<i>Consistency Ratio: 0.019221</i>											
<i>Distance from faults</i>											
										<i>Weight</i>	
9	0-400	1									0.300006
7	400-800	0.778	1								0.233336
5	800-1200	0.889	0.714	1						0.166666	
3	1200-1600	0.333	0.429	0.6	1					0.1	
1	1600-2000	0.111	0.143	0.2	0.333	1				0.33332	
1	2000-2400	0.111	0.143	0.2	0.333	1	1			0.33332	
1	2400-2800	0.111	0.143	0.2	0.333	1	1	1		0.33332	
1	2800-3200	0.111	0.143	0.2	0.333	1	1	1	1	0,33332	
1	3200-3600	0.111	0.143	0.2	0.333	1	1	1	1	1	0,33332
1	3600-4000	0.111	0.143	0.2	0.333	1	1	1	1	1	0,33332
<i>Consistency Ratio: 0.000032</i>											
<i>Distance from drainage</i>											
										<i>Weight</i>	
9	0-200	1									0.300006
7	200-400	0.778	1								0.233336
5	400-600	0.889	0.714	1						0.166666	
3	600-800	0.333	0.429	0.6	1					0.1	
1	800-1000	0.111	0.143	0.2	0.333	1				0.33332	
1	1000-1200	0.111	0.143	0.2	0.333	1	1			0.33332	
1	1200-1400	0.111	0.143	0.2	0.333	1	1	1		0.33332	
1	1400-1600	0.111	0.143	0.2	0.333	1	1	1	1	0.33332	
1	1600-1800	0.111	0.143	0.2	0.333	1	1	1	1	1	0.33332
1	1800-2000	0.111	0.143	0.2	0.333	1	1	1	1	1	0.33332
<i>Consistency Ratio: 0.000032</i>											
<i>NDVI</i>											
										<i>Weight</i>	
9	0.974026-0.231481	1									0.36001
7	0.231481-0.148438	0.778	1								0.280002
5	0.148438-0.045936	0.556	0.714	1						0.199995	
3	0.045936-0.151899	0.333	0.429	0.6	1					0.119997	

1	<i>0.151899-0.818182</i>	0.111	0.143	0.2	0.333	1				0.039996	
<i>Consistency Ratio: 0.000056</i>											
<i>Elevation</i>											
										<i>Weight</i>	
2	<i>500-600</i>	1								0.041665	
6	<i>600-700</i>	3	1							0.124999	
6	<i>700-800</i>	3	1	1						0.124999	
8	<i>800-900</i>	4	1.333	1.333	1					0.166664	
8	<i>900-1000</i>	4	1.333	1.333	1	1				0.166664	
9	<i>1000-1100</i>	4.5	1.5	1.5	1.125	1.125	1			0.187504	
9	<i>1100-1200</i>	4.5	1.5	1.5	1.125	1.125	1	1		0.187504	
<i>Consistency Ratio: 0.000023</i>											
<i>Density of spring water</i>											
										<i>Weight</i>	
2	<i>0-0.2</i>	1								0.05534	
2	<i>0.2-0.4</i>	1	1							0.05534	
4	<i>0.4-0.6</i>	2	2	1						0.110681	
5	<i>0.6-0.8</i>	2.5	2.5	1.25	1					0.138352	
6	<i>0.8-1</i>	3	3	1.25	1.2	1				0.166023	
8	<i>1-1.2</i>	4	4	2	1.6	1.333	1			0.221364	
9	<i>1.2-1.4</i>	4.5	4.5	2.5	1.8	1.5	1.125	1		0.2529	
<i>Consistency Ratio:0.001923</i>											
<i>Précipitation</i>											
										<i>Weight</i>	
3	<i>600</i>	1								0.125	
5	<i>700</i>	1.667	1							0.208	
7	<i>800</i>	2.333	1.4	1						0.292	
9	<i>900</i>	2.333	1.8	1.286	1					0.375	
<i>Consistency Ratio:0.000035</i>											
<i>Global matrix</i>											
										<i>Weight</i>	
9	<i>lithology</i>	1								0.147544	
8	<i>Slope angle</i>	0.889	1							0.131147	
7	<i>Slope aspect</i>	0.778	0.875	1						0.114754	
5	<i>Elevation</i>	0.556	0.625	0.714	1					0.081966	
5	<i>distance from drainage</i>	0.556	0.625	0.714	1	1				0.081966	
5	<i>distance from faults</i>	0.556	0.625	0.714	1	1	1			0.081966	
8	<i>Densité_ d'eau</i>	0.889	1	1.143	1.6	1.6	1.6	1		0.131147	
6	<i>NDVI</i>	0.667	0.75	0.857	1.2	1.2	1.2	0.75	1	0.098361	
8	<i>Precipitation</i>	0.889	1	1.143	1.6	1.6	1.6	1	1.333	1	0.131147
<i>Consistency Ratio: 0,000015</i>											



**4. RESULTS AND DISCUSSION:**

By overlaying the layers in GIS environment and using relative weights by AHP method, the final score LSI (Landslide Susceptibility Index) is computed by using Equation (2). The final results from calculated values of LSI, it was found its minimum value of 2.985, and a maximum value of 7.38, and standard deviation of 0.62. The LSI represents the relative susceptibility of a landslide occurrence. Therefore the higher the index, the more

susceptible the area is to landslides. These LSI values were then divided into five (5) classes based on the natural breaks range, which represents different zones in the landslide susceptibility map. These are Very High (VHS), High (HS), Moderate (MS), Low (LS), and Very Low (VLS) susceptibility zones (Fig. 3). The study concluded that East of Constantine, around Djebel Ouahche zones were very vulnerable to a landslide; around the NE and South of Aria were registered with low to very low susceptibility; and the rest of the area of moderate landslide potentiality (Fig.3).

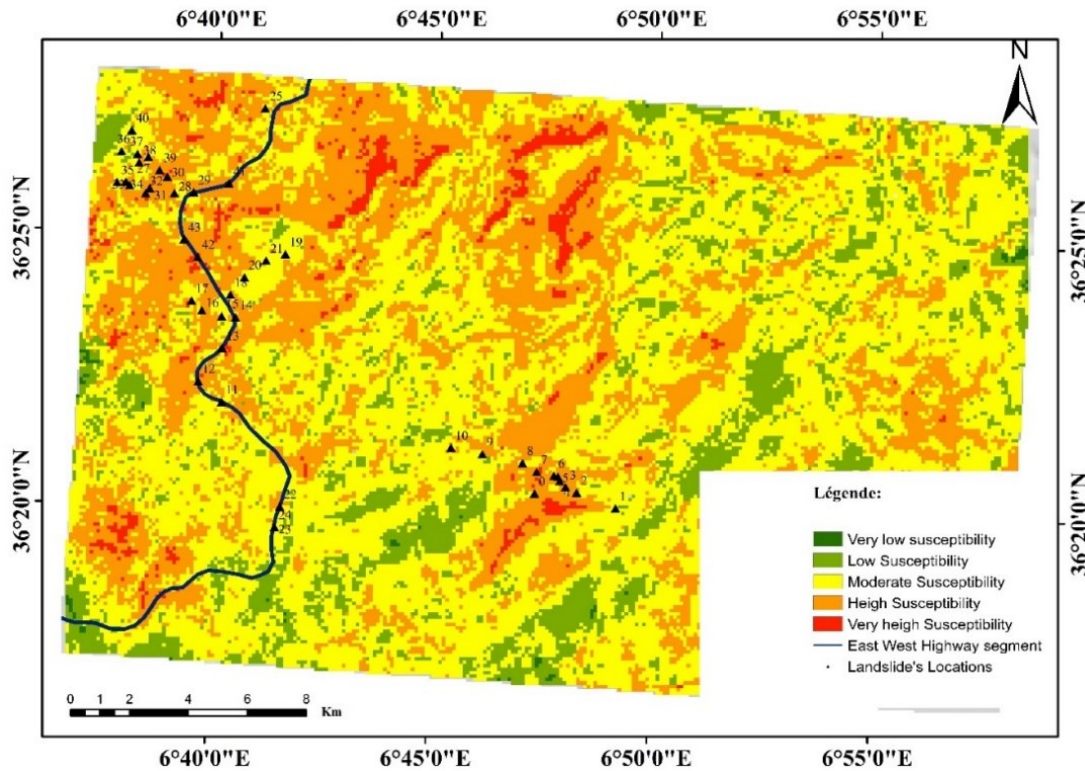


**Fig. 3** The landslide susceptibility map based on AHP with 43 known landslide location on the basis of natural break classification.

The study revealed that around 33% of the total area were classified as being in the VHS (2.1%) or HS (30.84%) landslide susceptibility zones, but they had represented by about 60% (Fig.4) of the landslides reference points (Table 4). Other classes MS, LS and VLS are represented, respectively, by 54.15%, 12.61%, and 0.3% of the total surface and only one landslide incidence (out of 43) in the LS zone. To check the validity of the results seen in Table 4 more quantitatively, the frequency ratio (FR) values for each class are also given. These values were calculated from the ratio of the percentage landslide occurrences and the percentage area coverage (for each class to the whole study area). The values begin from 0 continuing where relatively high ones (e. g. close to 0) indicate a higher chance of having landslides while low values (e.g., Close to 0) indicate a lower chance of having landslide over the area. FR equals (1) means the considered area is having an equal chance for landslide occurrence to that of the average value for the entire area. The FR values of 5.71 for the VHS zone and 1.55 for the HS zone involves the remarkable higher chance of

having landslide activities in these areas when compared to those of MS (0.66) and LS (0.31).

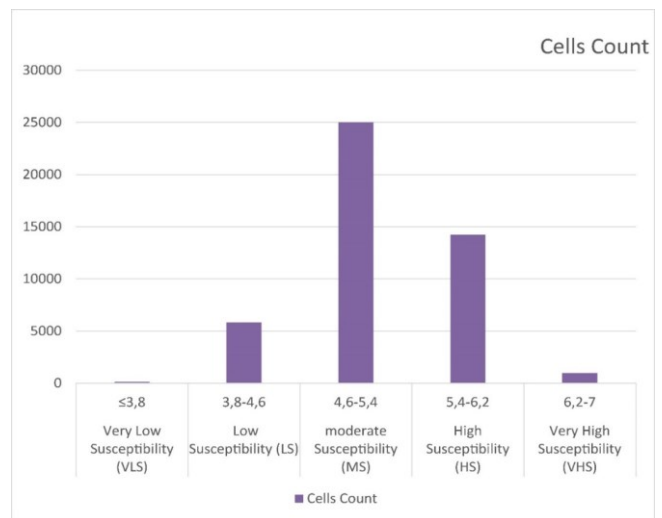


**Fig. 4** Pixel wise landslide susceptibility distribution.



**Table. 4: Allocation of the reference landslide points within the defined landslide susceptibility classes and the associated frequency ratio (FR) of each class.**

Susceptibility Class	Susceptibility Index	Area percentage	Landslide Point location number	Fréquency Ratio (FR)	Cells Count
Very Low Susceptibility (VLS)	≤3,8	0,30%	_ (0%)	0	139
Low Susceptibility (LS)	3,8-4,6	12,61%	1 (2,32%)	0,3172	5829
moderate Susceptibility (MS)	4,6-5,4	54,15%	13 (30,23%)	0,6648	25030
High Susceptibility (HS)	5,4-6,2	30,84%	23 (53,5%)	1,5564	14254
Very High Susceptibility (VHS)	6,2-7	2,10%	6 (14%)	5,7143	970

### 5. PERFORMANCE EVALUATION OF SUSCEPTIBILITY MAPS

To test the compatibility of the model and determination of its prediction ability, the area under the curve (AUC) method was used [40]. Generally, this approach compares the map of known landslides inventory with the susceptibility map. The range of the area under to ROC curve varies between 0 and 1 for a good fit, while values close to 1 being perfect and blow 0.5 defining a stochastic approximation [41]. The AUC is known as the best indicator to successfully differentiate possible landslide areas from regions with no predictable landslides [42]. In AUC curve assessment, Sensitivity (true-positive rate is the portion of false-positives out of the total actual positives) and 1-Specificity (false-positive rate is the portion of false-positives out of the total actual negatives) was performed for the model validation.

The AUC value is 0.61 and 0.59 (Fig 5), indicate the good ability of a function to correctly distinguish between failed and unfailed groups in the sample used for building the model, which means that the total success rate is 0.59.

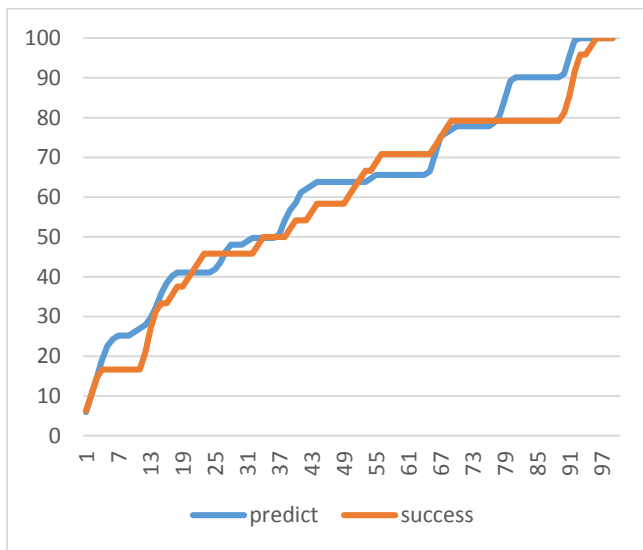


**Fig. 5** Receiver operating characteristics (ROC) curves representing quality of AHP model used.

### 6. CONCLUSION:

Landslide like other geological hazards is difficult to predict. However, it could be managed by the proceeding of the mapping of susceptibility to this phenomenon.

In this study, the analytical hierarchy process was used, and a susceptibility map is made for the east of Constantine which is located in the NE Algeria. To do that, nine (9) landslide causative factors were considered. Using AHP technique, an evaluation of these factors was applied, and factor weights and class weights were attributed to each of the associated factors. The most influencing factors to landslide activity according to their associated weights are precipitation (0.14), lithology (0.15) and slope angle (0.13).

The obtained susceptibility map give that the high and very high susceptible zones cover about 33% of the area while only 13% were classified as being the low and very low susceptible areas. About 54% of the area is moderate susceptible zone, the anthropogenic factor or trigger factors (heavy rainfall and earthquake) are enough of to reclassify the corresponding area in high susceptibility class. The map was verified using existing landslide location data based on the area under curve method from which the prediction accuracy of 61% was accomplished.

### REFERENCES

- [1] Bougdal R., Belhai D., Antoine P. (2007) Géologie détaillée de la ville de Constantine et ses alentours: une donnée de base pour l'étude des glissements de terrain. *Bull Serv Géol de l'Algérie*, 18(2):161-187.
- [2] Pincent B., Bougdal R., Panet M., Bentabet A. (2008). Le pont Sidi Rached à Constantine, Algérie : une culée dans un grand glissement de terrain. *Bull Serv Ge'ol de l'Algérie*, 19(3):197-215.
- [3] Machane, D., Bouhadad, Y., Cheikhounis, G., Chatelain, J., Oubaiche, E., Abbes, K., Guillier, B. and Bensalem, R. (2008). Examples of geomorphologic and geological hazards in Algeria. *Natural Hazards*, 45(2), pp.295-308.
- [4] Guemache, M., Chatelain, J., Machane, D., Benahmed, S. and Djadia, L. (2011). Failure of landslide stabilization measures: The Sidi Rached viaduct case (Constantine, Algeria). *Journal of African Earth Sciences*, 59(4-5), pp.349-358.
- [5] Manchar, N., Benabbas, C., Kacimi, M., Mimoun, A. and Bouaicha, F., (2012). Risque de glissements et aménagement: l'exemple d'un remblai autoroutier à Taffrent (NE de Constantine, Algérie nord orientale). 1<sup>er</sup> Congrès international de génie civil et d'hydraulique, Univ. 8 Mai 1945, Guelma, Algérie.
- [6] Bougdal, R., Larriere, A., Pincent, B., Panet, M. and Bentabet, A. (2013). Les glissements de terrain du quartier Bélouizdad, Constantine, Algérie. *Bulletin of Engineering Geology and the Environment*, 72(2), pp.189-202.

- [7] Bourenane, H., Bouhadad, Y., Guettouche, M. and Braham, M. (2014). GIS-based landslide susceptibility zonation using bivariate statistical and expert approaches in the city of Constantine (Northeast Algeria). *Bulletin of Engineering Geology and the Environment*, 74(2), pp.337-355.
- [8] Bourenane, H., Guettouche, M., Bouhadad, Y. and Braham, M. (2016). Landslide hazard mapping in the Constantine city, Northeast Algeria using frequency ratio, weighting factor, logistic regression, weights of evidence, and analytical hierarchy process methods. *Arabian Journal of Geosciences*, 9(2).
- [9] Varnes, D.J. 1984. Landslide Hazard Zonation: a Review of principles and practice. Natural Hazards. N°. 3. 1<sup>st</sup> ed. UNESCO, Paris, France, 63p.
- [10] Dai, F., Lee, C. and Ngai, Y. (2002). Landslide risk assessment and management: an overview. *Engineering Geology*, 64(1), pp.65-87.
- [11] Guzzetti, F., Reichenbach, P., Cardinali, M., Galli, M. and Ardizzone, F. (2005). Probabilistic landslide hazard assessment at the basin scale. *Geomorphology*, 72(1-4), pp.272-299.
- [12] Sharma, V. K., 2006. *Landslide hazard zonation: an overview of emerging techniques*. Journal of Engineering Geology, XXXIII, 73-80.
- [13] Guzzetti, F., Carrara, A., Cardinali, M., & Reichenbach, P. 1999. *Landslide hazard evaluation: a review of current techniques and their application in a multi scale study, Central Italy*. Journal of Geomorphology, 31, 181-216. Elsevier, London.
- [14] Carrara, A., Cardinali, M., Guzzetti, F., & Reichenbach, P. 1995. *GIS-Based techniques for mapping landslide hazard in Geographical Information System in Assessing Natural Hazards*. Dordrecht: Academic
- [15] Saha, A. K., Gupta, R. P., et Arora, M. K., 2002. *GIS based landslide hazard zonation in the Bhagirathi (Ganga) Valley, Himalayas*. International Journal of Remote Sensing, 23, 357-369pp.
- [16] Lee S. (2005). Application of logistic regression model and its validation for landslide susceptibility mapping using GIS and remote sensing data. *Int J Remote Sens* 7:1477-1491.
- [17] Van Westen, C. J., Castellanos Abella, E., et Sekhar, L. K., 2008. *Spatial data for landslide susceptibility, hazards and vulnerability assessment: an overview*. Engineering Geology, 102, 112-131.
- [18] Soeters, R., & Westen, C. J. 1996. *Slope instability recognition, analysis and zonation*. In A. K. Turner and R. L. Schuster (Eds), Landslides: Investigation and Mitigation. Transportation Research Board Special Report 249, 129-177.
- [19] Rowbotham D., Dudycha D. (1998). GIS modelling of slope stability in Phewa Tal watershed, Nepal. *Geophys J Roy Astron Soc* 26:151-170.
- [20] Lee S, Pradhan B. (2006). Probabilistic landslide hazard and risk mapping on Penang Island, Malaysia. *J Earth Syst Sci* 115:661-672.
- [21] Muthu, K., Petrou, M., Tarantino, C., and Blonda, P. (2008). Landslide Possibility Mapping Using Fuzzy Approaches. *IEEE Transactions on Geoscience and Remote Sensing*, 46(4): 1253-1265.
- [22] Pradhan, B. (2010). Remote Sensing and GIS-based landslide hazard analysis and cross validation using multivariate logistic regression model on three test areas in Malaysia. *Advances in Space Research*, 45, 1244-1256.
- [23] Pradhan, B. and Lee, S. (2010). Delineation of landslide hazard areas using frequency ratio, logistic regression and artificial neural network model at Penang Island Malaysia. *Environ Earth Sci* (2010) 60:1037-1054. DOI: 10.1007/s12665-009-0245-8.
- [24] Ma, F., Wang, J. Yuan, R, Zhao, H, Guo, J. (2013). Application of analytical hierarchy process and least square method for landslide susceptibility assessment along Zhong-Wu natural gas pipelines. *China Landslides Doi*, Doi: 10.1007/s10346-013-0402-8.
- [25] Kavzoglu, T., Sahin, E., and Colkensen I. (2013). Landslide susceptibility mapping using GIS based multi-criteria decision analysis, support vector machines and logistic regression. *Landslides*, doi:Doi: 10.1007/s10346-013-0391-7.
- [26] Guiraud, R. (1973). Evolution post-triasique de l'avant pays de la chaîne alpine en Algérie. D'après l'étude du bassin du Hodna et des régions voisines. Thèse de Doctorat Es Science, stratigraphie, Nice, 270pp.
- [27] Coiffait, P.-E., and VILA J M., 1977: Carte géologique de l'Algérie aux 1/50.000 feuilles d'El Aria avec notice explicative.
- [28] Coiffait, P.-E., 1992. Un bassin post-nappe dans son cadre structural: l'exemple du bassin de Constantine (Algérie nord-orientale). *Th. Doct. Etat Sci. Nat.*, Nancy, 1: 405.
- [29] Vila, J.-M., 1980. La chaîne alpine d'Algérie orientale et des confins algéro-tunisiens. Thèse Sc. Univ. Paris VI, 3 vol, 663 p., 199 fig., 40 pl., 7 pl.h.t.
- [30] Lahonder, J., C, 1987. Les séries ultratelliennes d'Algérie Nord-Orientale et les formations environnantes dans leur cadre structural, Paul Sabatier, Toulouse, France, 242 pp.
- [31] Raoult, J.F., (1974). Géologie du centre de la chaîne numidique (nord du constantinois, Algérie). , Paris, France, 156 pp.
- [32] Durand-Delga M(1969) Essai sur la structure du NE de la Berberie. *Bull Serv Carte geol Algérie* 39:89-181.
- [33] Crozier, M. J. (1986). *Landslides: causes, consequences and environment*, Croom Helm, London.
- [34] Coromina, J. (2000). Landslides and climate. Keynote lecture, in: *Proceeding of the 8<sup>th</sup> International Symposium on Landslides*, Balkema, Cardiff, 4, 1-33.

- [35] Tucker, C.J., Dregne, H.E. and Newcomb, W.W., 1991. Expansion and contraction of the Sahara Desert. *Science*, 253, pp.299-301.
- [36] Saaty, T.L. 1980. *The Analytical Hierarchy Process*. McGraw Hill, NY, 350p.
- [37] Malczewski, J. 1999. *GIS and Multi-Criteria Decision Analysis*. 1<sup>st</sup> ed. Jhon Wiley and Sons, NY, 392p.
- [38] Saaty, T. L. 1977. A scaling method for priorities in hierarchical structures. *Journal of mathematical psychology*, 15(3), 234-281.
- [39] Voogd, H. (1983). *Multicriteria Evaluation for Urban and regional Planning*. 1<sup>st</sup> ed. Pion Ltd., London, 367p.
- [40] Zweig MH, Campbell G (1993) Receiver-operating characteristics (ROC) plots. *Clin Chem* 39: 561–577.
- [41] Hanley JA, McNeil BJ (1983). A method of comparing the areas under receiver operating characteristic curves derived from the same cases. *Radiology* 148:839–843.
- [42] Lee S. (2005). Application of logistic regression model and its validation for landslide susceptibility mapping using GIS and remote sensing data. *Int J Remote Sens* 7:1477-1491.